

## Carbon Deposition by Micro Hollow Cathode Plasma Discharge

<sup>1</sup>Caniello R., <sup>2</sup>Russo V., <sup>1,2</sup>Dellasega D., <sup>1</sup>Causa F., <sup>1</sup>Cremona A., <sup>1,2</sup>Passoni M., <sup>1</sup>Ghezzi F.

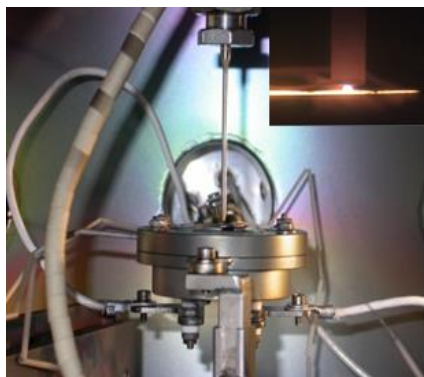
<sup>1</sup> *Plasma Physics Institute, CNR-ENEA-Euratom Association, Milan, Italy*

<sup>2</sup> *Dipartimento di Energia, Politecnico di Milano, Milan, Italy*

**Introduction:** Among many others, the micro-hollow cathode ( $\mu$ -HC) plasma discharge [1, 2] is an effective and efficient technique for applications in which high density of energetic radicals is required, for example, surface treatment, miniaturized etching and coating technology [3, 4]. In fact, unlike linear glow discharge mode,  $\mu$ -HC technique is characterized by highly energetic electrons ( $>10$ eV) trapped (pendulum effect [5]) in the radial electric field created in the cavity of the micro-cathode giving rise to a high plasma density (up to  $10^{16}$  cm<sup>-3</sup> [6]). Recently, deposition of polycrystalline diamond [7] and few layers graphene (FLG) [8] by direct current (DC)  $\mu$ -HC discharge, using methane (CH<sub>4</sub>) and molecular hydrogen (H<sub>2</sub>) as feeding gas, was demonstrated.

Here the authors present the variety of different carbon structures that can be deposited by low pressure (from 5 to 200 Torr) DC  $\mu$ -HC in H<sub>2</sub> and CH<sub>4</sub> environment on molybdenum (Mo) substrates: diamonds, carbon nanotubes (CNTs), few layers graphene and graphite coatings were grown at different substrate temperatures and working pressures. Carbon films were characterized by Scanning Electron Microscopy (SEM) and micro Raman spectroscopy. The results presented here demonstrate that  $\mu$ -HC plasma discharge is a very effective and versatile technique for the deposition of carbon materials.

**Experimental details:** Vacuum and gas supply system of the deposition plant is reported in a previous manuscript [9]. A 178  $\mu$ m inner diameter steel capillary tube is used as both gas inlet and discharge micro-hollow cathode (Fig. 1a). The anode is a furnace made of Mo which is used as both sample holder and substrate heater. The substrate is a polycrystalline Mo foil (0,05 mm, purity 99,9%) disk with a diameter of 12 mm which can be heated up 1200 °C by using a tungsten filament contained in the furnace. Two K-thermocouples placed directly on the substrate and at the furnace shield are used to monitor the temperature. The discharge occurs applying a negative voltage to the cathode and the discharge current and voltage can be measured by placing a resistor in series with the discharge. All the deposited spots presented here were grown up on Mo substrate with a deposition time of three hours and at CH<sub>4</sub>/H<sub>2</sub> flux ratio concentration of 0,005. The voltage supply ranges from 600 to 650 V giving rise to a current intensity comprises between 9 and 13 mA.



a)

| Sample | Working pressure (Torr) | Substrate Temperature (C°) | Note     |
|--------|-------------------------|----------------------------|----------|
| 1      | 10                      | 900                        | CNTs     |
| 2      | 70                      | 1000                       | FLG      |
| 3      | 100                     | 700                        | Graphite |
| 4      | 200                     | 800                        | Diamond  |
| 5      | 200                     | 905                        | Diamond  |
| 6      | 200                     | 1020                       | Diamond  |
| 7      | 200                     | 1100                       | Diamond  |

b)

**Figure 1:** a)  $\mu$ -HC plasma discharge setup. Inset: plasma discharge photograph. b) Deposition parameters table

The V-I characteristic of the discharge and the geometry of the  $\mu$ -HC have been discussed in a previous manuscript [9].

Before the deposition process, the substrate was carefully cleaned with hexane and deionised water and placed in the deposition chamber for several hours. A pre-discharge of pure  $H_2$  was performed for ten minutes before introducing  $CH_4$  gas in order to clean the substrate and to avoid temperature transients. In Fig. 1b the deposition parameters (working pressure and substrate temperature) of the samples selected for the present work are reported. SEM micrographs were performed using a ZEISS Supra System with an accelerating voltage of 5 kV. Raman spectroscopy was performed in the visible range with a Renishaw InVia micro Raman spectrometer using the blue line ( $\lambda = 457$  nm) of an Ar laser. Power was kept below 1 mW to avoid damage or modifications of the samples.

**Results:** As shown in Fig. 2 the spot deposition performed by  $\mu$ -HC plasma discharge has a diameter of about 0.7 mm and is totally confined in the region below the cathode. This clearly indicates that the deposition process is a plasma assisted chemical vapour deposition (CVD) and not a temperature assisted CVD. Choosing different process parameter it is possible to deposit different kinds of carbon films. In Fig. 3 SEM and Raman analysis of samples 1, 2 and 3 are shown. The three films exhibit very different morphologies: tangle of nanowires, carbon flakes and compact coating. Raman analysis allows to determine the nature of the deposited films. The bundle of nanowires observed in sample 1 reveals to be single-wall CNTs, showing the expected features known as  $G^+$ ,  $G^-$  and RBMs [10] in its Raman spectrum

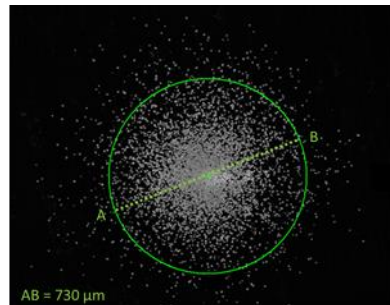


**Figure 2:** As-deposited spot by  $\mu$ -HC plasma discharge at 200 Torr,  $[CH_4]/[H_2] = 0,005$ ,  $T_{sub} = 900^{\circ}C$ , 3 h

(Fig. 3d). On the other hand the Raman spectrum of sample 2 (Fig. 3e) clearly shows the typical features of graphene systems, with the single lorentzian-shape second-order peak (2D) being much more intense than the G peak [8, 11]. Finally the sample 3 presents the well-known Raman spectrum (Fig. 3f) of polycrystalline graphite, with sharp D and G lines and multi-component second order peak (indicated as 2D) [11].

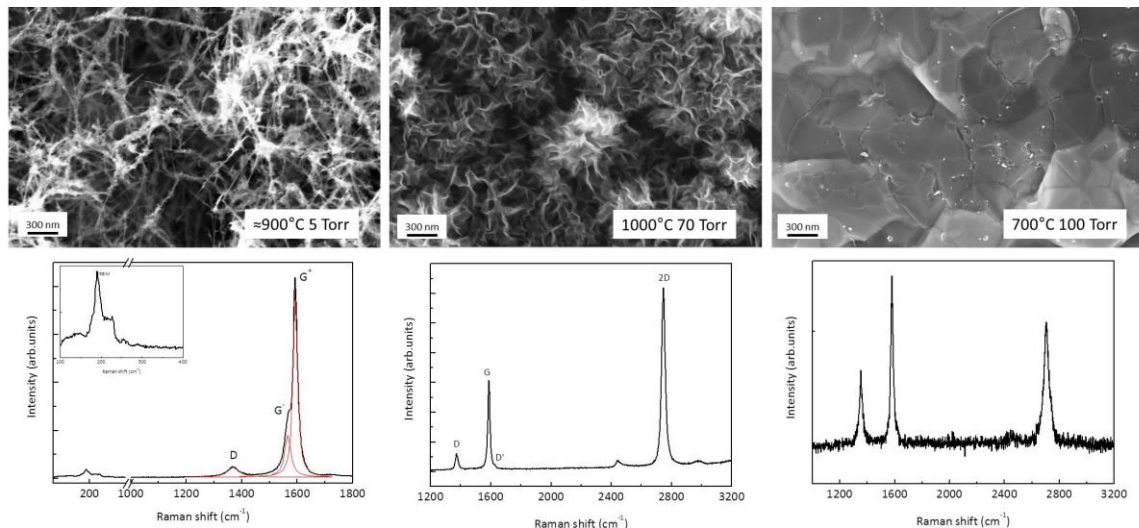


**Figure 3:** SEM micrographs (size bar equal to 300 nm) of carbon nanotubes (sample 1), graphene (sample 2) and graphite (sample 3) spot deposited by  $\mu$ -HC and the relative Raman spectra

A particularly interesting case is the possibility to deposit diamond films. In this frame, Figure 4 shows SEM images of sample 4, 5, 6 and 7 deposited at the same working pressure (200 Torr) but with different substrate temperatures, and the relative Raman spectra. Morphology of the samples changes varying substrate temperature. Sample 4 is constituted of nanometric spheroids (100 – 300 nm) where crystalline features are visible. Sample 5 appears continuous, with visible nanometric crystals (300 – 500 nm). Above 1000 °C, sample 6 appears to be constituted by micrometric grains, with nanometric features: different crystallographic oriented growths (100 and 111 planes) can be appreciated. When the temperature is raised at the highest investigated value (sample 7), the deposited spot again shows a nanostructured morphology even more open than at the lower temperatures. Despite morphology differences, all the samples deposited at 200 Torr show the typical Raman spectrum of diamond films [12]. This is characterized by a sharp peak at about  $1332\text{ cm}^{-1}$ , related to the first order diamond line, superimposed to large bands (indicated by D and G on the spectra), due to the  $\text{sp}^2$  carbon components always present in the bulk or at the grain boundaries of diamond films. Finally the two futures at about  $1150\text{ cm}^{-1}$  and  $1460\text{ cm}^{-1}$  are assigned to the  $\nu_1$  and  $\nu_3$  peaks of trans-polyacetylene present at grain boundaries [13]. The

quality of the diamond component of the films can be correlated with the width of the diamond peak and with the relative intensity between this peak and the contribution of the others non-diamond phases, resulting better at higher temperature.

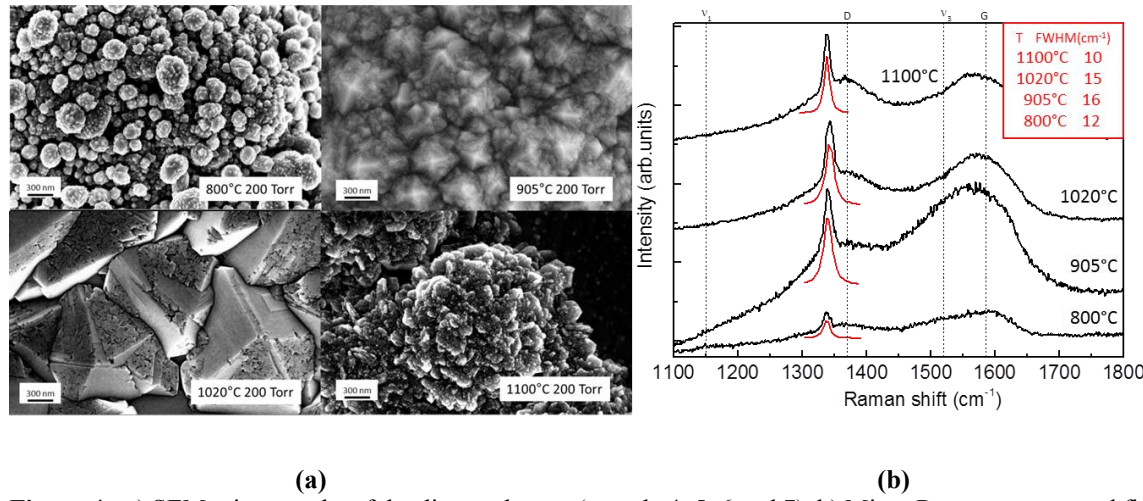


**Figure 4:** a) SEM micrographs of the diamond spots (sample 4, 5, 6 and 7). b) Micro Raman spectra and fitting lines of the diamond peaks. Inset: full width at half maximum of the fitting lines.

- [1] K. H. Schoenbach, R. Verhappen, T. Tessnow, F. E. Peterkin, W. W. Byszewski, *Applied Physics Letters* **68** (1), 13 (1996)
- [2] G. J. Kim, F. Iza, J. K. Lee, *Journal of Physics D: Applied Physics* **39**, 4386 (2006)
- [3] U. Kogelschatz, *Applications of Microplasmas and Microreactor Technology* **47**, 80 (2007)
- [4] R. M. Sankaran, K. P. Giapis, *Applied Physics Letters* **79**, 593 (2001)
- [5] G. J. Kim, J. K. Lee, *IEEE Transaction on Plasma Science* **36**, 1238 (2008)
- [6] K. H. Schoenbach, M. Moselhy, W. Sci, R. Bentley, *Journal of Vacuum Science & Technology A: Vacuum, Surfaces, and Films* **21**, 1260 (2003)
- [7] R. M. Sankaran, K. P. Giapis, *Journal of Applied Physics* **92**, 2406 (2002)
- [8] M. Passoni, V. Russo, D. Dellasega, F. Causa, F. Ghezzi, D. Wolverson, C. E. Bottani, *Journal of Raman Spectroscopy* **43**, 884 (2012)
- [9] F. Causa, F. Ghezzi, D. Dellasega, R. Caniello, G. Grossi, *Journal of Applied Physics* **112**, 123302 (2012)
- [10] A. Jorio, R. Saito, G. Dresselhaus, M.S. Dresselhaus, *Philosophical Transactions of the Royal Society A* **362**, 2311 (2004)
- [11] A. C. Ferrari, J. C. Meyer, V. Scardaci, C. Casiraghi, M. Lazzeri, F. Mauri, S. Piscanec, D. Jiang, K. S. Novoselov, S. Roth, A. K. Geim, *Physical Review Letters* **97**, 187401 (2006)
- [12] S. Prawer, R. J. Nemanich, *Philosophical Transactions of the Royal Society A* **362**, 2537 (2004)
- [13] A. C. Ferrari, J. Robertson, *Philosophical Transactions of the Royal Society A* **362**, 2477 (2004)